Extended Abstracts of the 2004 International Conference on Solid State Devices and Materials, Tokyo, 2004, pp. 782-783

C-8-3

Development of Simulation Method for Buried Oxide Formation of SIMOX Structure During Post-Implantation Thermal Annealing

Motoi Nakao[1], Koichi Sudoh[2], Hirofumi Iikawa[1], Hiroshi Iwasaki[2] and Katsutoshi Izumi[1]

[1] Research Institute for Advanced Science and Technology, Osaka Prefecture Univ.,
1-2, Gakuencho, Sakai, Osaka 599-8570, Japan
Phone: +81-72-254-9829 E-mail: nakao-m@riast.osakafu-u.ac.jp
[2] Institute of Science and Industrial Research, Osaka Univ.,
8-1 Mihogaoka, Ibaraki, Osaka 567-0047, Japan

1. Introduction

A separation by implanted oxygen (SIMOX) [1], one of successful technologies to fabricate silicon-on-insulator (SOI) structure, has superior characteristics of thickness uniformity of a top Si layer of SOI structure. Therefore, SIMOX technology is advantageous to the fabrication of SOI structure with an ultrathin top Si layer for further improvement of SOI device performance.

In current fabrication technology, a low-dose SIMOX, that employs a minimal oxygen dose that is followed by high temperature annealing, is commercially available [2]. On the other hand, low-dose SIMOX fabrication technology is restricted by a dose window [3], which is the range of an oxygen dose for the formation of a continuously buried oxide layer. While buried oxide islands are formed at doses below the dose window, Si islands are involved in buried oxide layers for excessive doses. Furthermore, the dose window depends on O^+ implantation energy [4], high-temperature annealing conditions [5] and substrate orientation [6].

Despite the technological importance and the interesting behavior of the formation of buried oxide layers, up to now few theoretical approaches for the dynamics of SiO_2 participation in an O^+ ion-implanted bulk Si have been performed. The understanding of pattern formation of SiO_2 precipitates is especially quite poor, and no established simulation technology for the process of SIMOX fabrication exists.

Therefore, we have developed a simulation method based on the Cahn-Hilliard model for pattern formation in SiO_2 participation during the thermal annealing of O^+ implanted Si wafers, and performed numerical simulations.

2. Simulation

In O^+ implanted bulk Si, oxygen atoms are in supersaturation, and thus during the annealing phase separation into SiO_2 and Si occurs. In this study we simply treat the phase separation as an evolution of oxygen concentration distribution in a Si matrix. The flow of oxygen is driven by the difference of free energy density that depends on the oxygen concentration. We introduce an order parameter φ corresponding to the oxygen concentration C, defined as $\varphi = C/C_0$, where C_0 is the oxygen concentration in SiO_2. The kinetics of such a redistribution process during which the order is conserved, can be described by a Cahn-Hilliard equation [7-8]. Assuming a simple form of a free energy function, $f = (1/2)(\nabla \varphi)^2 - \varphi^2 + \varphi^4$, we describe the time evolution of oxygen concentration distribution by

$$\frac{\partial \varphi(r,t)}{\partial t} = -L \frac{\delta \int dr \left[\frac{1}{2}(\nabla \varphi)^2 - \frac{A}{2}\varphi^2 + \frac{B}{4}\varphi^4 \right]}{\delta \varphi(r,t)}, \qquad (1)$$

where $\varphi(r,t)$ is the order parameter at the point r at time t, and L, A, and B are the phenomenological parameters. A polynomial expression in the right hand side of equation (1) is a factor inducing phase separation. A second-order differential of the order parameter or the oxygen concentration corresponds to a factor of surface energy, which is a driving force of the aggregation of SiO_2, as an Ostwald ripening [9-10]. We study how an oxygen concentration profile in O^+-implanted Si evolves during annealing by numerically integrating Eq. (1) in a three dimensional space. For simplicity, the simulation was conducted on the conditions that L is unity and A is equal to B.

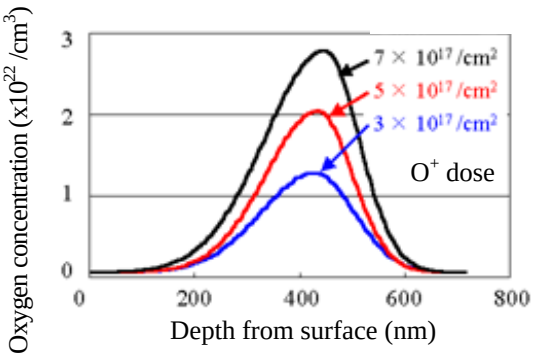

Fig. 1 Depth profiles of oxygen concentration in as-implanted Si substrate.

As an initial condition for the simulation, the depth profiles of oxygen concentration in as-implanted Si substrate, experimentally derived by spectroscopic ellipsometry [11], were used. By adding white noise to one-dimensional depth profiles of oxygen concentration for doses of 3x, 5x and $7x10^{17}$ /cm^2, shown in Fig.1, the initial

oxygen profile was expanded into a three-dimensional (3-D) distribution, and a dynamic 3-D simulation was conducted.

3. Results and discussion

Figures 2 (a), (b) and (c) show the cross-sectional transmission electron microscope (TEM) images of SIMOX structure after thermal annealing for doses of 3x, 5x and $7x10^{17}$ /cm^2, respectively. The thermal annealing was performed under 3%-O_2/Ar ambient for 4 hours at 1350^{o}C. In Fig. 2(b), a continuous buried oxide layer was observed for a dose of $5x10^{17}$ /cm^2. This result indicates that a dose of $5x10^{17}$ /cm^2 is within the dose window. On the other hand, for doses of 3x and $7x10^{17}$ /cm^2, discontinuous buried oxide layer and Si islands in buried oxide layer are observed as shown in Fig. 2 (a) and (c), respectively. These mean that doses of 3x and $7x10^{17}$ /cm^2 are smaller and larger than the dose window, respectively.

Figures 2 (d), (e) and (f) show the cross-sectional images obtained by our simulation. A gray scale corresponds to the oxygen concentration or the order parameter from 0 to 1. For each dose, stable images for t=9000 is employed. As shown in Fig. 2 (e), continuous buried oxide layer is obtained for a dose of $5x10^{17}$ /cm^2, although an interface between the top Si and buried oxide layers is slightly rougher than the experimental one. In Fig. 2 (d) and (f) corresponding to doses of 3x and $7x10^{17}$ /cm^2, buried oxide island and Si region (islands) in buried oxide layer are recognized, respectively.

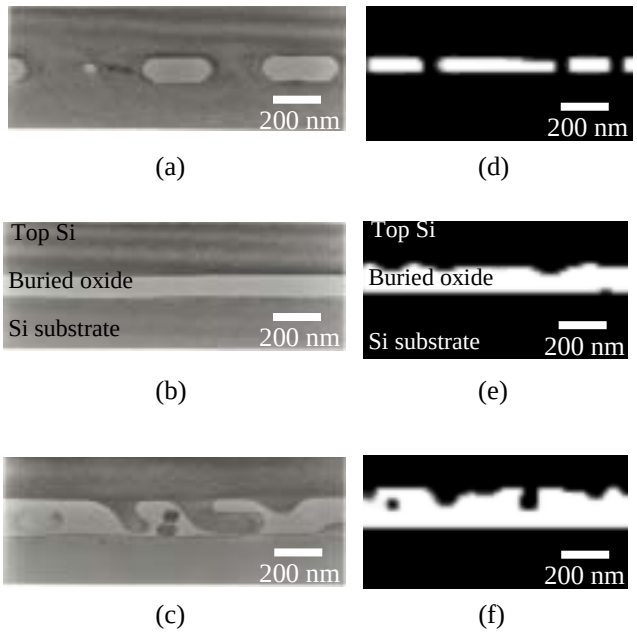

Fig. 2 Cross-sectional images of SIMOX substrates. (a), (b) and (c) are experimental results by TEM; (d), (e) and (f) are simulated results. Oxygen doses correspond to $3x10^{17}$/cm^2 for (a) and (d), $5x10^{17}$/cm^2 for (b) and (e), and $7x10^{17}$/cm^2 for (c) and (f).

These three images of Fig. 2 (d), (e) and (f) are similar to the experimental ones of Fig. 2 (a), (b) and (c). These results indicate that using numerical simulations based on the Cahn-Hilliard model, we have successfully reproduced the experimentally observed buried oxide formation of SIMOX substrate that is dependent on an initial oxygen concentration profile. Therefore, using this simulation, an aspect of buried oxide layer of SIMOX structure can be predicted for such various process conditions as O^+-implantation energies and doses; that is, dose-window for various O^+-implantation energies can be extracted. Furthermore, this simulation is also applicable for studying the formation mechanisms of the buried oxide layer of SIMOX structures.

4. Conclusions

We have developed a simulation method for buried oxide layer formation of SIMOX structure during thermal annealing after oxygen implantation into Si. The precipitation of SiO_2 in oxygen implanted Si substrates is numerically simulated, introducing a Cahn-Hilliard equation for the evolution of oxygen concentration distribution in a Si matrix. We have found that different initial depth profiles of oxygen causes different types of profiles of domain structures distinguished as a continuous oxide layer, an array of discontinuous oxide islands, and an oxide layer including Si islands. Our simulation well reproduces the SIMOX structures observed experimentally for different oxygen doses. These results indicate that our simulation method enables to extract the dose window for continuous oxide layer formation as well as to study the formation mechanism of buried oxide layer of SIMOX substrate by post-implantation thermal annealing.

Acknowledgements

This work was financially supported in part by New Energy Industrial Technology Development Organization (NEDO).

References

[1] K. Izumi, M. Doken and H. Ariyoshi: Electron. Lett. **14** (1978) 593.
[2] A. Matsumura, I. Hamaguchi, K. Kawamura, T. Sasaki, S. Takayama, and Y. Nagatake, Microelectron. Eng. **66** (2003) 400.
[3] S. Nakashima and K. Izumi: J. Mater. Res. **8** (1993) 523.
[4] M. Chen, X. Wan, J. Chen, X. Liu , Y. Dong, Y. Yu , X. Wang, Appl. Phys. Lett. **80** (2002) 880.
[5] A. Ogura, J. Electrochem. Soc. **145** (1998) 1735.
[6] H. Iikawa, M. Nakao, and K. Izumi, (unpublished).
[7] J. W. Cahn and J. E. Hilliard, J. Chem. Phys. **28** (1958) 258.
[8] Y. Oono and S. Puri, Phys. Rev. A **38** (1988) 434.
[9] J. Burke, in *The Kinetics of Phase Transformation in Metals*, (Pergamon, Oxford, 1965) 103.
[10] C. Jaussaud, J. Margail, J. Stoemenos, and M. Bruel, Mat. Res. Soc. Symp. **107** (1988) 17.
[11] H. Iikawa, M. Nakao, B. Gruska, and K. Izumi, J. Electrochem. Soc. **151** (2004) G373.